

## Generic equations for pattern formation in evolving interfaces

**Mario Castro<sup>1,4</sup>, Javier Muñoz-García<sup>2</sup>, Rodolfo Cuerno<sup>2</sup>,  
Maria del Mar García Hernández<sup>3</sup> and Luis Vázquez<sup>3</sup>**

<sup>1</sup> Grupo Interdisciplinar de Sistemas Complejos (GISC) and Grupo de Dinámica No Lineal (DNL), Escuela Técnica Superior de Ingeniería (ICAI), Universidad Pontificia Comillas, E-28015 Madrid, Spain

<sup>2</sup> Departamento de Matemáticas and GISC, Universidad Carlos III de Madrid, E-28911 Leganés, Spain

<sup>3</sup> Instituto de Ciencia de Materiales de Madrid (CSIC), E-28049 Madrid, Spain

*New Journal of Physics* **9** (2007) 102

Received 4 October 2006

Published 25 April 2007

Online at <http://www.njp.org/>

doi:10.1088/1367-2630/9/4/102

**Abstract.** We present a general formalism which allows us to derive the evolution equations describing one-dimensional (1D) and isotropic 2D interface-like systems, that is based on symmetries, conservation laws, multiple scale arguments, and exploits the relevance of coarsening dynamics. Our approach becomes especially significant in the presence of surface morphological instabilities and allows us to classify the most relevant nonlinear terms in the continuum description of these systems. The formalism applies to systems ranging from eroded nanostructures to macroscopic pattern formation. In particular, we show the validity of the theory for novel experiments on ion plasma erosion.

<sup>4</sup> Author to whom any correspondence should be addressed.

**Contents**

<b>1. Introduction</b>	<b>2</b>
<b>2. Theory</b>	<b>3</b>
2.1. Nonconserved dynamics. . . . .	3
2.2. Conserved dynamics. . . . .	6
<b>3. Results</b>	<b>7</b>
3.1. Application to 1D systems . . . . .	7
3.2. Application to novel experiments . . . . .	9
<b>4. Discussion and conclusions</b>	<b>10</b>
<b>Acknowledgments</b>	<b>11</b>
<b>References</b>	<b>11</b>

**1. Introduction**

Many surfaces and interfaces, which are very different in nature and occur at very different length scales, produce interfaces which are startlingly similar. This similarity stems from the competition between stabilizing and destabilizing physical mechanisms that are insensitive to the specific value of the interface height  $h(x, t)$  (this function provides the height of an interface above position  $x$  on a one-dimensional (1D) substrate, at time  $t$ ). Namely, such mechanisms are invariant under global height translations of the form  $h(x, t) \rightarrow h(x, t) + \xi$ , with  $\xi$  an arbitrary constant (shift symmetry [1]). For instance, interesting ((sub)micrometric) surface features develop by growth or erosion using various techniques, such as electrochemical deposition (ECD) [2], chemical vapour deposition (CVD) [3], ion beam sputtering (IBS) [4] or molecular beam epitaxy (MBE) [5], but remarkably also in macroscopic systems, such as aeolian sand dunes [6] or underwater (vortex) ripples in sand [7].

For cases in which dynamical instabilities are irrelevant or absent, the shift symmetry has been argued to induce scale-invariant surface morphologies in the presence of noise. This is the *generic scale invariance* [8] associated with the universality classes [9] of kinetic roughening. However, the situation differs in the presence of morphological instabilities, that are the landmark of pattern formation. In these cases, if the height field is seen as a measure of the *amplitude* of perturbations around a reference homogeneous state, the conservation law associated with the shift symmetry leads to a large-scale instability [10]. This might prevent a unified description by means of a universal equation, such as the Ginzburg–Landau equation is for the case of short-wavelength instabilities [10, 11]. Thus, although the systems mentioned above are seemingly governed by similar equations, a general theory of evolving interfaces in which patterns arise is still lacking. Actually, it seems that for every experimental system a specific theory needs to be developed.

In this paper, we present a general formalism for pattern formation in 1D and isotropic 2D surfaces, that relates to previous approaches in the theory of dynamic scaling of rough interfaces [1, 12, 13], systematically exploiting the formulation of the interface evolution within the assumption of a (generalized) relaxational dynamics. Through symmetries and multiple scale arguments, our approach helps to understand why some effective equations presenting a morphological instability appear almost ubiquitously in the experimental systems mentioned

above. Our method enables classification of the most relevant nonlinear terms for these systems, and stresses the relevance of the phenomenon of coarsening to their continuum description. We have also performed some experiments on ion plasma erosion to explore nontrivial implications of our theory. Moreover, we have applied it to other relevant and diverse fields, ranging from thin film production to surface patterns in macroscopic systems, such as fluid waves or some granular systems.

In principle, we consider that the evolution of  $h$  is local and takes the form  $\partial_t h = \mathcal{G}(\{h\}) + \eta$ , where  $\{h\}$  stands for  $h$  and its spatial derivatives, and  $\eta$  is a noise term that we will neglect hereafter. Previous phenomenological proposals for the functional  $\mathcal{G}$  have been built upon geometry arguments [12] or upon symmetry and conservation requirements [9]. In the first case, the evolution is governed by the local curvature and its derivatives along the interface. This excludes contributions to  $\mathcal{G}$  that are due to, e.g. anisotropies [14]. Likewise, the second approach can be misleading. For instance, if one considers nonconserved interface dynamics under the shift symmetry, namely, if  $\mathcal{G}$  cannot be derived from a current, one could naively drop terms like  $\frac{1}{2}\partial_x^2 h^2$  (because it can be written as  $\partial_x j$ ) or  $h\partial_x^2 h$  (because it is not shift invariant). However,  $\mathcal{G}$  could contain a term proportional to  $(\partial_x h)^2$ , namely, the sum of both terms. This may be innocuous in the presence of generic scale invariance, but not in the presence of instabilities; therefore, a systematic method is needed to classify the terms in the equation.

## 2. Theory

### 2.1. Nonconserved dynamics

We proceed by studying separately systems with nonconserved and conserved dynamics. As in [1, 13], we assume that the dynamics of the systems is relaxational in a generalized sense (namely, with a nonconstant mobility). Although this assumption is not strictly necessary, it greatly clarifies the interpretation of the coefficients of the nonlinear terms below. Hence,

$$\partial_t h = -\Gamma(\{h\}) \frac{\delta F(\{h\})}{\delta h}, \quad (1)$$

where  $\Gamma$  and  $F$  are a function and a functional of the height field and its spatial derivatives, respectively. Hereafter, we restrict  $\{h\}$  to be  $\{h, \partial_x h, \partial_x^2 h, \partial_x^3 h\}$ .<sup>5</sup>

If the relaxation rate  $\Gamma$  is a constant, symmetry under global shifts forbids any explicit dependence of  $F$  on  $h$ ; otherwise, what needs to be independent of  $h$  is the right-hand side of equation (1). Consequently, one can write (note our difference in sign convention from [1]):

$$\mathcal{F}(h, \partial_x h, \partial_x^2 h, \partial_x^3 h) = e^{-sh} \mathcal{F}_1(\partial_x h, \partial_x^2 h, \partial_x^3 h), \quad (2)$$

$$\Gamma(h, \partial_x h, \partial_x^2 h, \partial_x^3 h) = e^{sh} \Gamma_1(\partial_x h, \partial_x^2 h, \partial_x^3 h), \quad (3)$$

where the height scale  $s$  is the generator of the group of symmetry under translations in  $h$ , and we have written  $F(\{h\}) = \int \mathcal{F}(\{h\}) dx$ . We have to emphasize that  $F(\{h\})$  will be a proper Lyapunov

<sup>5</sup> Dependence on higher order derivatives, e.g.  $\partial_x^4 h$ , only changes  $\beta$  and  $K$  in equation (6), but modifies neither the nonlinear terms nor the general discussion.

functional for equation (1)—in the sense that dynamics minimizes  $F(\{h\})$ —only provided the nonconstant mobility  $\Gamma(\{h\})$  is a positive definite function. This will not be the case for many of the systems we study, in which the mobility depends on the height field and its derivatives in a way that does not necessarily preserve positiveness (see equation (4) below); such a dependence will in general break the *global* relaxational character of the dynamics described by (1).

Close to the instability threshold, we can assume that local slopes are small,  $|\partial_x h| \ll 1$ , and we can expand  $\Gamma_1$  and  $\mathcal{F}_1$  in power series. Therefore,

$$\Gamma_1 = \sum_{i,j,k} \gamma^{(ijk)} (\partial_x h)^i (\partial_x^2 h)^j (\partial_x^3 h)^k, \quad (4)$$

$$\mathcal{F}_1 = \sum_{i,j,k} f^{(ijk)} (\partial_x h)^i (\partial_x^2 h)^j (\partial_x^3 h)^k. \quad (5)$$

Using these expansions in equation (1), we obtain a list of terms compatible with the shift symmetry. As mentioned above, in general this dependence eliminates the relaxational character of the dynamics, with the result that the *formal* Lyapunov functional no longer governs the asymptotic behaviour of the system. The resulting equations are quite involved. Hence, we first consider the linear terms. We will include the most relevant nonlinear terms later. Thus, we find

$$\partial_t h = V_\perp + V_\parallel \partial_x h + \nu \partial_x^2 h + \beta \partial_x^3 h - K \partial_x^4 h + \dots, \quad (6)$$

where

$$V_\perp = s\gamma f, \quad V_\parallel = s\gamma^{(100)} f, \quad (7)$$

$$\nu = s\gamma^{(010)} f + 2s\gamma f^{(010)} + 2\gamma f^{(200)}, \quad (8)$$

$$\beta = s\gamma^{(001)} f, \quad K = -2\gamma f^{(020)} + 2\gamma f^{(101)}, \quad (9)$$

and  $\gamma \equiv \gamma^{(000)}$ ,  $f \equiv f^{(000)}$ . The real part of the dispersion relation for single mode solutions of equation (6),  $h(x, t) \sim \exp[\omega_q t + ikx]$ , reads  $\text{Re}(\omega_q) = -\nu q^2 - Kq^4$ ; consequently, a morphological instability arises if  $\nu < 0$  and  $K > 0$ . The characteristic length scale for the ensuing pattern will be roughly given by the wavelength of the mode maximizing  $\omega_q$ , namely,  $l = 2\pi\sqrt{2K/|\nu|}$ . When nonlinear terms are incorporated into equation (6), this length scale can grow giving rise to a *coarsening* process [15], that will help us to identify which nonlinear contributions are actually playing a role in the full dynamics. Close to the instability threshold  $\nu = 0$ , equation (8) can be written as  $\nu = -2\gamma f^{(200)}(s - s_c)/s_c \equiv -2\gamma f^{(200)}\epsilon$ , with  $\epsilon$  a small dimensionless parameter, and  $s_c = -2\gamma f^{(200)}/(\gamma^{(010)} f + 2\gamma f^{(010)})$ . Note that the length scale  $l$  diverges as  $\epsilon^{-1/2}$  in the limit  $\epsilon \rightarrow 0$ , as  $K$  is  $s$ -independent, according to equation (9). Consequently, we can rescale length, time and height as  $x \rightarrow x/l$ ,  $t \rightarrow t/l^z$  and  $h \rightarrow h/l^\alpha$ , and, using the multiple scales method, look for the most relevant nonlinear term. As in the theory of dynamic scaling [9], we find that this term is the celebrated Kardar–Parisi–Zhang (KPZ) nonlinearity  $\lambda(s, s^2)(\partial_x h)^2$ , with  $\lambda(s, s^2) \equiv s\gamma f^{(200)} - s^2\gamma f^{(010)} - s\gamma f^{(200)}$ , where the notation

stresses the polynomial dependence of  $\lambda$  on  $s$ . The KPZ interface equation is a paradigm of non-equilibrium systems, so that its appearance within our present (formally, ‘equilibrium’) formulation may seem paradoxical. However, as first shown by [1], thanks to the dependence of the generalized mobility on the height field, it is indeed possible to derive explicitly the KPZ equation for simple choices of  $\mathcal{F}_1$  and  $\Gamma_1$  in (2) and (3). For instance, if

$$\Gamma_1 = \gamma + \gamma^{(200)}(\partial_x h)^2, \quad \mathcal{F}_1 = f + f^{(200)}(\partial_x h)^2 + f^{(020)}(\partial_x^2 h)^2,$$

one obtains the KPZ equation in the form

$$\partial_t h = s\gamma f + 2\gamma f^{(200)}(\partial_x^2 h) - 2\gamma f^{(020)}(\partial_x^4 h) + (sf\gamma^{(200)} - s\gamma f^{(200)})(\partial_x h)^2, \quad (10)$$

where we have dropped higher order nonlinearities that are irrelevant in the hydrodynamic limit but that otherwise follow from the *formally* relaxational form of equation (1). However, as long as we do not keep all terms that follow from  $\Gamma_1$  and  $\mathcal{F}_1$ , the variational character is broken, as expected by the fact that the Kuramoto–Sivashinsky (KS) equation, for instance, is known to exhibit spatiotemporal chaos, and this would contradict the fact that the equation would be obtained from a variational principle.

For many experimental situations, however, this limit may lie beyond practical reach [16, 17], in which case the final structure depends crucially on subdominant terms that must be included in the evolution equation in order to capture essential features of the original nonlinear system. This can be done within our multiple scale framework: for instance, the ratio between  $(\partial_x h)^2$  and  $(\partial_x h)(\partial_x^2 h)$  scales as

$$\frac{(\partial_x h)^2}{(\partial_x h)(\partial_x^2 h)} \sim l,$$

so that, in the limit  $l \rightarrow \infty$ , the former term dominates the latter. This calculation can be reproduced for every term resulting in the series expansion, with the following results for the first correcting terms, in order of relevance:

$$\begin{aligned} \lambda_{110}(1, s, s^2)(\partial_x h)(\partial_x^2 h), \quad \lambda_{300}(1, s, s^2)(\partial_x h)^3, \quad \lambda_2(1, s)\partial_x^2(\partial_x h)^2, \\ \lambda_{101}(s)(\partial_x h)(\partial_x^3 h), \quad \lambda_{210}(1, s, s^2)(\partial_x h)^2(\partial_x^2 h), \quad \lambda_{400}(s, s^2)(\partial_x h)^4, \end{aligned} \quad (11)$$

where

$$\lambda_{110} = sf\gamma^{(1,1,0)} + 2s\gamma^{(1,0,0)}f^{(0,1,0)} + 2\gamma^{(1,0,0)}f^{(2,0,0)} + 3s\gamma f^{(1,1,0)} + 3s^2\gamma f^{(0,0,1)} + 6\gamma f^{(3,0,0)}, \quad (12)$$

$$\lambda_{300} = s(-s\gamma^{(1,0,0)}f^{(0,1,0)} - \gamma^{(1,0,0)}f^{(2,0,0)} - s^2\gamma f^{(0,0,1)} - s\gamma f^{(1,1,0)} - 2\gamma f^{(3,0,0)} + \gamma^{(3,0,0)}f), \quad (13)$$

$$\lambda_{101} = 5s\gamma f^{(0,2,0)}/2 - 5s\gamma f^{(1,0,1)}/2 + s\gamma^{(1,0,1)}f - s\gamma^{(0,2,0)}f/2 - s\gamma^{(0,1,0)}f^{(0,1,0)} - \gamma^{(0,1,0)}f^{(2,0,0)} \quad (14)$$

$$\begin{aligned} \lambda_2 &= s\gamma f^{(0,2,0)}/2 - 3s\gamma f^{(1,0,1)}/2 + 3s\gamma^{(0,2,0)}f/2 + s\gamma^{(0,1,0)}f^{(0,1,0)} + \gamma^{(0,1,0)}f^{(2,0,0)} \\ \lambda_{210} &= -2s^2[f^{(0,1,0)}\gamma^{(0,1,0)} - 3f^{(0,0,1)}\gamma^{(1,0,0)} + \gamma(2f^{(0,2,0)} - 6f^{(1,0,1)})] + 4f^{(2,0,0)}\gamma^{(2,0,0)} \\ &\quad + s(6\gamma^{(1,0,0)}f^{(1,1,0)} - 2\gamma^{(0,1,0)}f^{(2,0,0)} + 4f^{(0,1,0)}\gamma^{(2,0,0)} \\ &\quad + 8\gamma f^{(2,1,0)} + 2f\gamma^{(2,1,0)}) + 12\gamma^{(1,0,0)}f^{(3,0,0)} + 24\gamma f^{(4,0,0)}, \end{aligned} \quad (15)$$

$$\lambda_{400} = s(-s\gamma^{(2,0,0)} f^{(0,1,0)} - \gamma^{(2,0,0)} f^{(2,0,0)} - s^2\gamma^{(1,0,0)} f^{(0,0,1)} - s\gamma^{(1,0,0)} f^{(1,1,0)} - 2\gamma^{(1,0,0)} f^{(3,0,0)} - s^2\gamma f^{(1,0,1)} - s\gamma f^{(2,1,0)} - 3\gamma f^{(4,0,0)} + f\gamma^{(4,0,0)}), \quad (16)$$

and we have used that  $(\partial_x^2 h)^2 = [\partial_x^2(\partial_x h)^2 - \partial_x h \partial_x^3 h] / 2$ .

An example is provided by the so-called dissipation-modified Korteweg–de Vries equation,

$$\partial_t h = \nu \partial_x^2 h + \beta \partial_x^3 h - K \partial_x^4 h + \lambda (\partial_x h)^2 + \lambda_{110} \partial_x^2 h \partial_x h, \quad (17)$$

proposed [18] as the generic amplitude equation for weakly nonlinear waves, appearing in contexts ranging from Marangoni or Rayleigh convection to periodic waves in binary fluid mixtures (see references in [18]). In our surface context, it describes for example the dynamics of (1D) ion-sputtered interfaces under oblique incidence, see references in [19]. In general, while the term  $(\partial_x h)^2$  dominates asymptotically, it interrupts coarsening [20, 21]. This is actually the case for equation (17). Consequently, eventual coarsening of the pattern must be due to other terms in equation (11). For instance, if one adds the  $\lambda_2$  term in equation (11) to the right-hand side of equation (17), (interrupted) coarsening indeed occurs [22]. Further details and examples are provided below in section 3.1.

## 2.2. Conserved dynamics

In the case of conserved dynamics for the interface, we can write [1]

$$\partial_t h = \partial_x \left( \Gamma(\{h\}) \partial_x \frac{\delta F(\{h\})}{\delta h} - j_{\text{nr}} \right). \quad (18)$$

The assumption of (generalized) relaxational dynamics is now stronger than in the nonconserved case, the operator between  $\Gamma$  and  $\delta F/\delta h$  constrains the form of the possible terms in a multiple scale expansion (see below). In order to make the problem as general as possible, we need to include the non-relaxational current,  $j_{\text{nr}}$ , in the right hand side of equation (18). The origin of this type of current has been widely discussed for example in the context of mound formation in homoepitaxial growth [5, 23]. Assuming that  $j_{\text{nr}}$  depends only on derivatives of  $h$  in the form

$$j_{\text{nr}} = \sum_{i,j,k} J^{(ijk)} (\partial_x h)^i (\partial_x^2 h)^j (\partial_x^3 h)^k, \quad (19)$$

and using equation (4)–(5) as above, equation (18) becomes

$$\partial_t h = \nu^c \partial_x^2 h + \beta^c \partial_x^3 h - K^c \partial_x^4 h + \lambda_{110}^c (\partial_x h) (\partial_x^2 h) + \lambda_2^c \partial_x^2 (\partial_x h)^2 + \lambda_{210}^c (\partial_x h)^2 (\partial_x^2 h), \quad (20)$$

where all the coefficients in equation (20) depend on  $\gamma^{(ijk)}$ ,  $f^{(ijk)}$  and  $J^{(ijk)}$ . Thus,

$$\nu^c = s^2 \gamma f - J^{(1,0,0)}, \quad (21)$$

$$\beta^c = -J^{(0,1,0)}, \quad (22)$$

$$K^c = J^{(0,0,1)} + 2s\gamma f^{(0,1,0)} + \gamma f^{(2,0,0)}, \quad (23)$$

$$\lambda_{110}^c = 2s^2\gamma^{(1,0,0)} f - J^{(2,0,0)}, \quad (24)$$

$$\lambda_2^c = s(s\gamma^{(0,1,0)} f + 4s\gamma f^{(0,1,0)} + 2\gamma f^{(2,0,0)})/2, \quad (25)$$

$$\lambda_{210}^c = s^2(-3s\gamma f^{(0,1,0)} - 3\gamma f^{(2,0,0)}/2 + 3\gamma^{(2,0,0)} f/2). \quad (26)$$

An interesting result derived from the above equations is that, whenever  $j_{\text{nr}} = 0$ , the condition for unstable growth reads  $\epsilon \propto s^2$ , so that power counting (with  $l \sim \epsilon^{-1/2}$ ,  $t \sim l^z$  and  $h \sim l^\alpha$ ) provides terms which give a divergent scaling of the local slope, namely,  $|\partial_x h|$  scales with a positive power of  $l$ . This means that the small-slope approximation breaks down and the expansions above are no longer valid, in analogy, e.g. to the so-called superrough scaling in the context of surface kinetic roughening [9], occurring specifically in the case of conserved dynamics. In these conditions, detailed knowledge of system characteristics is needed and a strongly nonlinear analysis must be performed in order to obtain the correct interface equation, as in [24].

### 3. Results

Thus far, we have derived the most general and relevant interface equations compatible with the shift symmetry. We proceed by testing the validity of the theory and, more importantly, its capability to identify the right terms of the evolution equation in each situation, based on experimental or theoretical evidence, through our procedure that accounts for conservation, symmetries and coarsening in systems where a surface instability is present. To illustrate this method of analysis, we discuss several 1D examples of systems—with length scales ranging from microscopic to macroscopic—for each type of dynamics, both nonconserved and conserved. Moreover, some of the examples correspond to isotropic 2D surfaces.

#### 3.1. Application to 1D systems

To begin with, we consider nonconserved growth of nanometric sized patterns by IBS. In this technique, the surface of a solid target is isotropically bombarded with a flux of energetic ions. Experimentally, a typical length scale develops at early times and is seen to grow later (coarsening). The system is not conserved due to the mass loss as a consequence of the bombarding process. Finally, the experimentally obtained surfaces do not develop steep slopes (so a small slope approximation is well justified). With these ingredients in mind, our theory predicts that the evolution equation for these systems must contain the term proportional to  $\lambda$  due to the nonconserved nature of the experiment and terms  $\lambda_2$ ,  $\lambda_{101}$  and  $\lambda_{210}$  due to the presence of coarsening. Hence,

$$\partial_t h = \nu(\partial_x^2 h) - K(\partial_x^4 h) + \lambda(\partial_x h)^2 + \lambda_2 \partial_x^2(\partial_x^2 h) + \lambda_{101}(\partial_x h)(\partial_x^3 h) + \lambda_{210}(\partial_x h)^2(\partial_x^2 h). \quad (27)$$

Consistent with the above expectation, a hydrodynamic theory of erosion has been reported [20] which couples a fast field describing the density of mobile particles at the surface with a slow one which corresponds to the observed experimental surface. This theory allows us to relate experimental magnitudes to the corresponding equation parameters and, precisely, leads to equation (27).

At intermediate length scales (microns to millimetres), we can take growth by ECD [2], where the surface of an aggregate grows by incorporation of cations from a solution. The assumption of locality above is reasonable for a small sticking probability, i.e. if the cations do not attach to the first visited surface site but are, rather, allowed to diffuse further until aggregation occurs. The cation flux at any surface point is isotropic, hence the system is reflection ( $x \rightarrow -x$ ) symmetric. Finally, the characteristic length of the unstable structures observed experimentally does not grow in time, i.e. there is no coarsening. These data suggest that surface dynamics for ECD is described by the KS equation, namely,  $V_{\parallel} = \beta = 0$ , due to the reflection symmetry, and that all the terms in equations (11) are negligible, compatible with the absence of coarsening. The same scenario is observed in surface growth by CVD [3]. Indeed, the KS equation has been derived explicitly for both ECD and CVD from constitutive equations, in agreement with our results [16].

Our final example of nonconserved interface growth is taken from surface instabilities in fluids due to surface tension gradients (see [25] for a comprehensive reference), a standard example being provided by Marangoni–Bénard convection [26]. In this system, a thin fluid layer is subject to an external transverse temperature gradient, there being nonconserved fluxes that implement the dissipation in the system. When heating from below, a convective instability sets in whose spatial characteristics do not coarsen in time. This instability leads to travelling waves on the free surface of the system which break the  $x \rightarrow -x$  reflection symmetry. An asymptotic study of the corresponding hydrodynamic problem leads to the equation [25, 26]

$$\partial_t h = \nu(\partial_x^2 h) - K(\partial_x^4 h) + \lambda(\partial_x h)^2 + \lambda_{110}(\partial_x h)(\partial_x^2 h), \quad (28)$$

in agreement with the general expectation from our approach under the constraints considered.

As an important example of conserved interface dynamics at nanometric scales, we consider the growth by MBE of surfaces that are vicinal to a high symmetry crystalline orientation [27]. In this type of experiments, the molecules incorporated from the chamber arrive isotropically at the surface (and hence reflection symmetry is fulfilled), the relevant 1D interface being given by the location of the step separating one terrace from an adjacent one. Under conditions in which the rate of adatom evaporation from the terrace is vanishingly small, the dynamics is conserved. It is precisely in this case that the small slope approximation has been seen to break down [24], as for equation (18) for  $j_{nr} = 0$ . However, if adatom desorption occurs on the terraces, the system becomes nonconserved and the relevant interfacial description is provided by the KS equation [28], as expected from our above arguments.

Finally, an example of conserved interface growth in a macroscopic system is provided by the formation of macroscopic ripples in aeolian sand dunes [12]. In this case, the wind direction breaks the reflection symmetry and, as the surface dynamics at the sand bed is conserved due to the conservation of the number of sand grains, one would expect equation (20) to hold as the relevant continuum equation. Indeed, this has been shown to be the case within the so-called hydrodynamic approach to pattern formation in these systems [12].

The results in this section, as well as some other experimental systems that can be analysed along similar lines, are summarized in table 1, where we provide references to the experimental



**Table 1.** Physical examples. Nonconserved (NC), conserved (C), strongly-nonlinear (SN). RS means reflection symmetry ( $x \rightarrow -x$ ), and ‘Coars.’ is coarsening.

System	Type	RS	Coars.	Nonlinearities	Exp.	Theor.
ECD/CVD	NC	Yes	No	$\lambda$	[29]	[16]
IBS	NC	Yes	Yes	$\lambda, \lambda_{2,101, 210}$	[30]	[20]
Thin films	NC	Yes	Yes	$\lambda, \lambda_2$	[31]	[32]
Fluid waves	NC	No	No	$\lambda, \lambda_{110}$	[25]	[25]
MBE (singular)	C	Yes	Yes	$\lambda_{210}^c$	[27]	[5]
MBE (vicinal)	C	Yes	No	SN	[27]	[24]
Sand ripples	C	No	Yes	$\lambda_{2, 110, 210}^c$	[33]	[6]
Vortex ripples	C	Yes	Yes	SN	[34]	[7]

observations and to theoretical derivations compatible with our conclusions. We provide the reader with broader references when connection with specific experiments is less unambiguous.

### 3.2. Application to novel experiments

The examples in the last subsection show how, based on general considerations, one can construct a general equation in good agreement with current specific theories. Notwithstanding, we want to emphasize the wide range of generality of our method by applying it to novel experiments on ion plasma erosion. Thus, a Si(100) wafer (2 inches diameter) was immersed in a magnetically confined argon plasma at a pressure of  $5 \times 10^{-3}$  mbar. Under these conditions the flux of incoming ions on the central part of the wafer is mainly isotropic. The only parameter changed in the experiments was the immersion (i.e. sputtering) time. After the sputtering process, the central part of the wafer was analysed by atomic force microscopy operating in tapping mode with a silicon cantilever. We plot two snapshots of the surface taken at 3 h (figure 2(a)) and 6 h (figure 2(b)). Moreover, we have measured a nonzero coarsening exponent  $n = 0.53 \pm 0.02$  in  $\ell \sim t^n$ ,  $\ell$  being the mean cell diameter. Given the isotropy of the system, we can generalize our results above to this case. Out of the most relevant subdominant terms in equation (11) (once generalized to two dimensions) compatible with isotropy,  $\lambda_2$  [21, 32] and  $\lambda_{210}$  [35, 36] are known in the literature to induce coarsening behaviour when taken in combination with  $\lambda_{100}$  and a KS dispersion relation. Extensive numerical simulations [22] show that the term  $\lambda_{101}$  also induces coarsening, but the term  $\lambda_{400}$  does not. Hence, thus far we are left with an equation of the following form:

$$\partial_t h = -\nu \nabla^2 h - K \nabla^4 h + \lambda (\nabla h)^2 + \lambda_2 \nabla^2 (\nabla h)^2 + \lambda_{101} \nabla h \cdot \nabla (\nabla^2 h) + \lambda_{210} (\nabla h)^2 (\nabla^2 h). \quad (29)$$

From the experimental data we can extract some quantitative information about the coefficients in equation (29). Thus, a closer inspection of the experimental surface cross-section (figure 1) reveals that *cell* shape can be approximated by

$$(\nu^2 / K \lambda_{210})^{1/2} \log(\cosh [(2K/\nu)^{1/2} x]), \quad (30)$$

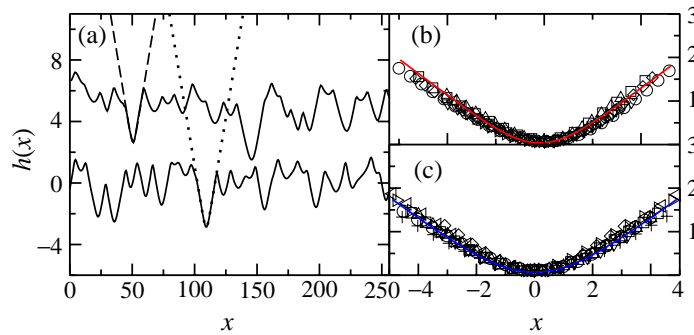


**Figure 1.** (a) Cross-section of figure 2(a) morphologies, both numerical (lower curve) obtained with  $\nu = 1$ ,  $K = 0.11$ ,  $\lambda_{210} = 0.052$  and  $\lambda = -0.05$  and experimental (upper curve). Dashed line stands for a fit of the experimental cell shape to equation (30), which allows us to obtain the parameters used in the numerical simulations. Dotted line is a translation of the dashed line to stress the self-consistency of the parameter extraction. (b) Fit to equation (30) of seven *valleys* extracted from top curve in figure 1(a). Red solid line stands for the dashed and dotted lines in figure 1(a). (c) Fit to equation (30) of eight *valleys* extracted from bottom curve in figure 1(a). Blue solid line stands for the dashed and dotted lines in figure 1(a).

which is a solution of equation (29) in 1D with  $\lambda_2 = \lambda_{101} = 0$  (and, therefore, approximately valid for large cells in the isotropic 2D case). This suggests that  $\lambda_2$  and  $\lambda_{101}$  are negligible, since large values for them would rather lead to parabolic cells [20].

Consequently, equation (29) reduces effectively to

$$\partial_t h = -\nu \nabla^2 h - K \nabla^4 h + \lambda (\nabla h)^2 + \lambda_{101} \nabla h \cdot \nabla (\nabla^2 h), \quad (31)$$

the so-called convective Cahn–Hilliard equation [36]. For short times (linear regime), the typical length scale allows determination of the  $K/\nu$  value, while the remaining parameters are estimated by trial and error in order to improve the resemblance to the experimental morphologies. Results of such numerical simulations are compared with experiments in figure 2 showing an excellent agreement between them. Thus, the small panels (upper insets) display two snapshots of the numerical integration of equation (31) and the large panels the equivalent results from experiments.

#### 4. Discussion and conclusions

Although table 1 is not meant to be exhaustive, it leads to some general observations. As anticipated above, the occurrence of coarsening is an important property in guiding the identification of the appropriate nonlinear terms of a given system. This phenomenon was associated with the seeming inability to describe patterns that are stable both in wavelength and amplitude by means of local height equations [7, 15]. However, there may exist now counterexamples [20, 21] for this shortcoming, at least for an order range that is much larger than the single cell size. As a consequence, the task of determining the necessary and sufficient

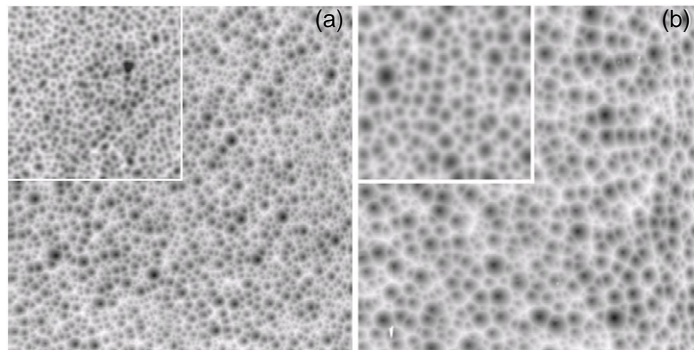


**Figure 2.** (a) Ion plasma eroded Si(100) at  $t_e = 3$  h. Inset: numerical simulation of equation (31) at  $t_s = 35$  with  $\nu = 1$ ,  $K = 0.11$ ,  $\lambda_{210} = 0.052$  and  $\lambda = -0.05$ . The lateral size of the image is  $50 \mu\text{m}$ . (b) Ion plasma eroded Si(100) at  $t_e = 6$  h. Inset: simulation as in (a) for  $t_s = 70$ . The lateral size of the image is  $50 \mu\text{m}$ .

conditions for coarsening [15], as well as the possible values (universality classes) for the coarsening exponent  $n$ , remains to be completed, lying outside the scope of this paper. Note that, once coarsening occurs, the fact that it *interrupts* [15] or not, and the value of exponent  $n$ , both depend on the type of leading and subleading nonlinearities that appear in the evolution equation. Hence, these provide additional criteria in order to propose a continuum description for a given physical system; nevertheless it can be the case that two different subleading terms lead to the same coarsening exponent value, such as in the case of  $\lambda_2$  and  $\lambda_{210}$ , both of them yielding  $n = 1/2$  [35, 37]. Moreover, system dimensionality and the (possibly related) relevance of noise may influence the value of the coarsening exponent in the corresponding universality classes.

In summary, we have provided a systematic method to obtain and classify the relevant nonlinear terms in interfacial systems which present morphological instabilities and the shift symmetry. Besides, we have applied our method to some reported systems in the literature as well as to novel experiments on ion plasma erosion performed for this purpose.

## Acknowledgments

This work has been partially supported by MECD (Spain), through grants nos. FIS2006-12253-C06-01, FIS2006-12253-C06-03, FIS2006-12253-C06-06, and the FPU programme (JM-G).

## References

- [1] Hentschel H G E 1994 *J. Phys. A: Math. Gen.* **27** 2269
- [2] Schwarzacher W 2004 *J. Phys.: Condens. Matter* **16** R859
- [3] Jensen F and Kern W 1991 *Thin Film Processes II* ed J LVossen and W Kern (Boston: Academic)
- [4] Valbusa U, Boragno C and Buatier de Mongeot F 2002 *J. Phys.: Condens. Matter* **14** R8153
- [5] Politi P, Grenet G, Marty A, Ponchet A and Villain J 2000 *Phys. Rep.* **324** 271
- [6] Valance A and Rioual F 1999 *Eur. Phys. J. B* **10** 543
- [7] Krug J 2001 *Adv. Complex Syst.* **4** 353

- [8] Grinstein G 1995 *Scale Invariance, Interfaces and Non-Equilibrium Systems* ed A McKane, M Droz, J Vannimenus and D Wolf (New York: Plenum)
- [9] Barabási A-L and Stanley H E 1995 *Fractal Concepts in Surface Growth* (Cambridge: Cambridge University Press)
- [10] Nepomnyashchy A A 1995 *Physica D* **86** 90
- [11] Cross M C and Hohenberg P C 1993 *Rev. Mod. Phys.* **65** 851
- [12] Csehók Z, Misbah C and Valance A 1999 *Physica D* **128** 87
- [13] López J M, Castro M and Gallego R 2005 *Phys. Rev. Lett.* **94** 166103
- [14] Golovin A A, Davis S H and Nepomnyashchy A A 1999 *Phys. Rev. E* **59** 803
- [15] Politi P and Misbah C 2004 *Phys. Rev. Lett.* **92** 090601  
Politi P and Misbah C 2006 *Phys. Rev. E* **73** 036133
- [16] Cuerno R and Castro M 2001 *Phys. Rev. Lett.* **87** 236103
- [17] Cuerno R and Vázquez L 2004 *Advances in Condensed Matter and Statistical Physics* ed E Korutcheva and R Cuerno (New York: Nova Science)
- [18] Bar D E and Nepomnyashchy A A 1995 *Physica D* **86** 586
- [19] Makeev M, Cuerno R and Barabási A-L 2002 *Nucl. Instrum. Methods Phys. Res. B* **197** 185
- [20] Castro M, Cuerno R, Vázquez L and Gago R 2005 *Phys. Rev. Lett.* **94** 016102  
Castro M and Cuerno R 2005 *Phys. Rev. Lett.* **94** 139601  
Muñoz-García J, Castro M and Cuerno R 2006 *Phys. Rev. Lett.* **96** 086101
- [21] Muñoz-García J, Cuerno R and Castro M 2006 *Phys. Rev. E* **74** 050103 (R)
- [22] Muñoz-García J 2007 Invariancia de Escala y Formación de Patrones en la Erosión de Superficies *PhD Thesis* Universidad Carlos III de Madrid
- [23] Krug J, Plischke M and Siegert M 1993 *Phys. Rev. Lett.* **70** 3271
- [24] Pierre-Louis O, Misbah C, Saito Y, Krug J and Politi P 1998 *Phys. Rev. Lett.* **80** 4221  
Gillet F, Pierre-Louis O and Misbah C 2000 *Eur. Phys. J. B* **18** 519
- [25] Colinet P, Legros J C and Velarde M G 2001 *Non-linear Dynamics of Surface-Tension-Driven Instabilities* (Berlin: Wiley)
- [26] Garazo A N and Velarde M G 1991 *Phys. Fluids A* **3** 2295
- [27] Michely T and Krug J 2004 *Islands, Mounds and Atoms* (Berlin: Springer)
- [28] Karma A and Misbah C 1993 *Phys. Rev. Lett.* **71** 3810
- [29] Schilardi P L, Azzaroni O, Salvarezza R C and Arvia A J 1999 *Phys. Rev. B* **59** 4638  
Léger C, Elezgaray J and Argoul F 2000 *Phys. Rev. E* **61** 5452
- [30] Facsko S, Dekorsy T, Koerdt C, Trappe C, Kurz H, Vogt A, and Hartnagel H L 1999 *Science* **285** 1551  
Gago R, Vázquez L, Cuerno R, Varela M, Ballesteros C and Albella J M 2001 *Appl. Phys. Lett.* **78** 3316
- [31] Mayr S G, Moske M and Samwer K 1999 *Phys. Rev. B* **60** 16950
- [32] Raible M, Linz S J and Hänggi P 2001 *Phys. Rev. E* **64** 031506 and references therein
- [33] Rioual F 2002 Etude de quelques aspects du transport olien: processus de saltation et formation des rides *PhD Thesis* Université de Rennes
- [34] Stegner A and Wesfreid J E 1999 *Phys. Rev. E* **60** R3487
- [35] Emmott C L and Bray A J 1996 *Phys. Rev. E* **54** 4568
- [36] Golovin A A, Nepomnyashchy A A, Davis S H and Zaks M A 2001 *Phys. Rev. Lett.* **86** 1550
- [37] Raible M, Linz S J and Hänggi P 2000 *Phys. Rev. E* **62** 1691

Q1